TECHNICAL DESIGN OF THE BASELINE GUN FOR THE NLS PROJECT

Jang-Hui Han*, Houcheng Huang, Shivaji Pande, Diamond Light Source, Oxfordshire, UK

Abstract

The UK's proposed New Light Source (NLS) project has the baseline specification of FEL photon energies ranging up to 1 keV and a repetition rate of 1.1 kHz. In order to fulfil this specification, an injector consisting of a normal conducting L-band (1.3 GHz) photocathode gun and a superconducting L-band (1.3 GHz) cavity module has been designed. The gun should operate with high RF peak power up to 4.6 MW and high RF average power up to 77 kW. Therefore, the gun temperature rise and the cavity deformation should be minimised. For such a high power operation, the RF power transmission through the coupler must be maximised. In this article, technical issues of the thermal behaviour of the gun and the RF design of the coupler are discussed.

INTRODUCTION

For the UK's proposed New Light Source (NLS) project [1], the injector has to provide electron beams with 1.1 kHz repetition rate. At the same time, the beams must satisfy the requirement for the SASE or seeded FEL processes. The injector will consist of a normal conducting L-band (1.3 GHz) gun and a linac module with 8 TESLA type superconducting L-band (1.3 GHz) cavities. The normal conducting gun will operate with pulsed mode with about 15 μs pulse length at 1.1 kHz repetition rate while the superconducting cavities will operate with continuous wave (CW) mode. The first injector design has been reported [2] and the parameters satisfied the NLS beam quality requirements [3]. Since the RF duty factor of the gun will be 1.65%, which is higher than that of the DESY gun for the European XFEL [4], a lower RF peak power should be used for the NLS gun in order to keep the RF average power in an acceptable range. Nevertheless, the average RF power in the NLS gun will be higher than both the FLASH gun [5] and the European XFEL gun. The temperature control of the NLS gun may therefore be challenging and so its thermal behaviour must be simulated in detail.

The NLS gun will have a coaxial coupler like DESY guns [6]. The coupling characteristics between the cavity and the door-knob coupler have been investigated in order to find an optimal configuration.

In this article the thermal analysis of the cavity carried out with ANSYS [7] and the RF analysis of the coupler with CST Microwave Studio [8] are discussed.

THERMAL BEHAVIOUR OF RF GUN

The main cavity body will be made from oxygen-free high conductivity (OFHC) copper. As the surface current induced by the magnetic field during RF operation is not uniform over the cavity, the temperature rise will also be non-uniform. In this gun design, the cooling-water channel is distributed over the cavity so that the cavity temperature rise and the non-uniformity are minimised [9]. The photocathode plug and the outer jacket of the cooling channel will be made from molybdenum and stainless steel, respectively. The stainless steel jacket helps to suppress the cavity deformation during RF operation.

The gun should operate with 50 MV/m RF amplitude [2]. If the cavity temperature is kept at room temperature, about 4.3 MW RF peak power would be needed for 50 MV/m (Table 1). However, during RF operation the cavity temperature will rise to about 60°C (see Fig. 1) and therefore the surface conductivity of the cavity will decrease. At the higher temperature, RF power needed for the RF amplitude will be about 4.6 MW (Table 1). The cavity temperature rise during the RF operation should be controlled by water temperature regulation in order to keep the cavity in resonance at 1.3 GHz.

Table 1: Cavity quality factor (Q) and RF power (P) required to achieve 50 MV/m at the cathode for different cavity temperatures

Temp	20°C	30°C	40°C	50°C	60°C	70°C	80°C
Q	22965	22527	22113	21720	21348	21019	20682
P (MW)	4.292	4.376	4.458	4.538	4.617	4.686	4.762

When the gun cavity operates with 4.6 MW RF peak power, 15 μs pulse length and 1.1 kHz repetition rate, the RF average power is about 77 kW. In the previous report [9], the thermal behaviour has been analysed for 70 kW power. Since the NLS baseline repetition rate was chosen as 1.1 kHz, a new analysis was done.

To improve thermal and deformation behaviour of the cavity, the cooling-water channel position and back plane area in the vicinity of the cathode plug were modified against the design reported in [9]. However, the shape of the cooling-water channel is unchanged. The RF power dissipation in the cavity inner surface was calculated with SUPERFISH [10]. In order to get the power dissipation at different location in the cavity inner surface, the surface was divided into small areas. Then, the power dissipation information was implemented into ANSYS for thermal analysis. We started with the steady state analysis; 77 kW RF average power dissipation was applied to the cavity inner surface. The cooling water temperature was set to 30°C. The heat transfer coefficient of cooling water was set as 9.1 $mW/mm^2 \cdot °C$ that was calculated according to 2 m/s water speed through the cooling channel. The gun outer surface was assumed to be cooled by 22°C air. The air cooling effect was negligible compared to the water

*jang-hui.han@diamond.ac.uk

cooling. An analysis with coarse mesh was conducted before a finer mesh with over 1 million nodes and 440,000 solid elements was generated. The result of the steady state analysis is shown in Fig.1. The hottest region was on the central iris plane where the power dissipation per area is high and the cooling-water channel is locally missing (see Fig. 1 in Ref [9]). In that region, the temperature increased up to 74.1°C. The photocathode plug region was quite hot, 68.9°C, even though there was very small RF power dissipation in the area. The reason is that the area does not have good thermal contact to the cooling-water.

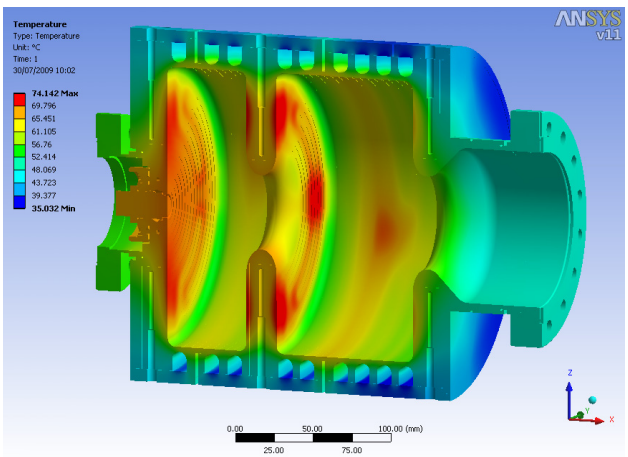

Figure 1: Temperature distribution over the cavity for 77 kW RF average power. The maximum temperature is 74.1°C when 30°C cooling water is used.

In addition to the average cavity temperature rise caused by the RF average power, extra heating during an RF pulse produces further temperature rise. Because the heat transfer from the cavity inner surface to the body is not fast enough compared to the RF power dissipation to the surface, the surface temperature may rise quickly during the RF pulse. After the pulse, the surface temperature monotonically falls until the next pulse induces a temperature rise again. This pulse temperature rise may result in further cavity deformation and possibly the cavity quality factor change. If the temperature rise by pulse heating is about 40°C, the cavity may be damaged due to material fatigue [11].

The surface temperature rise, ΔT_s, during pulse length, τ, for dissipated RF power density, P_{RF}, is scaled as [11, 12, 13, 14]

$$\Delta T_s = \frac{2P_{RF}\sqrt{\tau}}{\sqrt{\pi\rho k C_\varepsilon}}, \qquad (1)$$

where $\rho = 8.93 \times 10^3$ kg/m^3, $k = 391$ W/m·K and $C_\varepsilon = 385$ J/kg·K are the material density, the heat capacity and the specific heat for OFHC copper in this model, respectively.

Surface temperature rise for different RF pulse lengths can be analytically estimated with Eq. 1. In order to validate the equation, a transient thermal analysis was also carried out with the same mesh as for the steady state analysis using ANSYS. The temperature distribution resulting from the steady state analysis with the average RF power was employed as the initial condition. The resulting temperature distribution after the 15 μs RF pulse with 4.6 MW peak is shown in Fig. 2. At the hottest point, the temperature rise was about 1.3°C (from 74.1°C to 75.4°C). The temperature at the cathode was changed by only 0.03°C. A comparison between analytic values with Eq.1 and numerically calculated ones with ANSYS is shown in Fig. 3; we can see a very good match of the analytic and numerical values though the agreement for short pulses is not as good as for longer pulses. However, for the NLS gun, the temperature rise during the 15 μs pulse would be only a few degrees and therefore serious material fatigue and significant quality factor change are not expected.

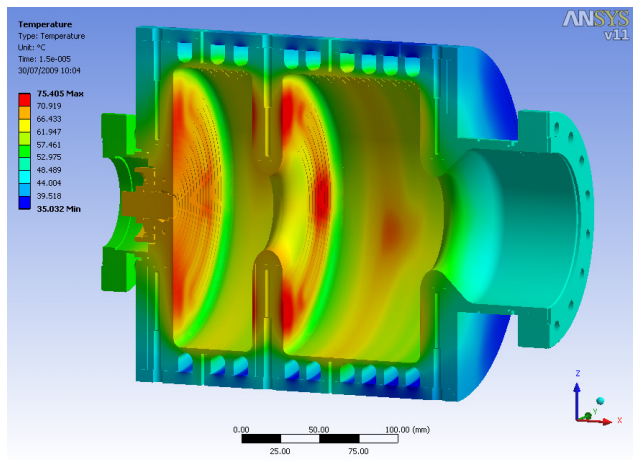

Figure 2: Temperature distribution over the cavity at the end of a 15 μs 4.6 MW pulse in addition to the 77 kW RF average power. An additional temperature rise of 1.3°C at the maximum temperature region takes place from the steady state temperature in Fig. 1.

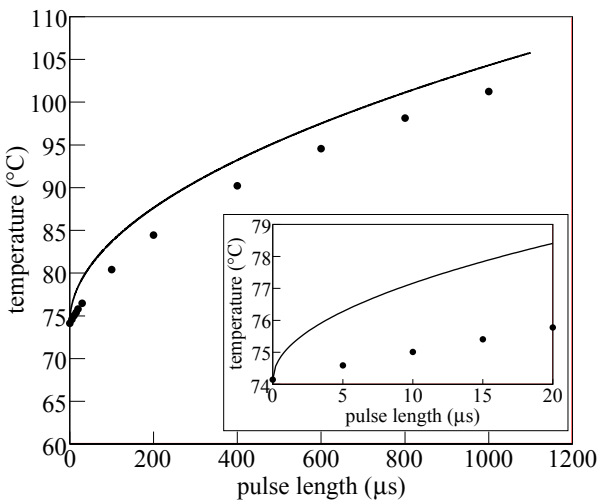

Figure 3: Temperature rise at the hottest point on the inner surface of the cavity for different 4.6 MW RF pulse length. The results analysed with ANSYS are shown as black points. An analytic estimation with Eq. 1 is shown as a solid line. In the small box in the figure, the temperature variation up to 20 μs RF pulse is shown.

For the above calculations we used a 4.6 MW peak power because this results in an average temperature of about 60°C which is therefore consistent with achieving the required 50 MV/m at the cathode (Table 1). However, at some locations in the iris and the back plane the temperature is about 75°C where the surface current is high. On the other hand, the temperature at the cylinder tube and at the corner between the tube and the iris is lower than 60°C over a large area where the surface current is also high. The non-uniform surface temperature distribution may change the required RF peak power and finally change the cavity temperature. However, we estimate that the required increase in RF peak power is within 1% and further cavity temperature rise within 0.4°C. We will carry out more detailed simulations to confirm this in the future.

RF COUPLER OPTIMISATION

To maximise the cooling capacity of the cavity as discussed in the previous section and to make the RF field axisymmetric, a coaxial coupler like the DESY gun [6] will be used for the NLS gun (see Fig. 4). The door-knob was modified from the DESY design so that the distance between the inner antenna tube and the end plate opposite to the waveguide is exactly λ/4, where λ is the RF wavelength. The RF characteristics with the coupler were studied numerically.

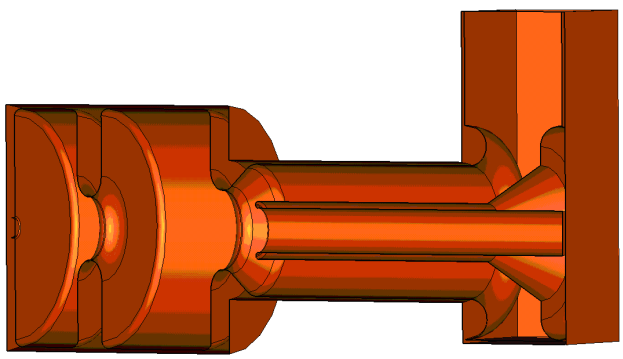

Figure 4: Cutaway view of the CST Studio model for the L-band gun. The gun cavity and the coaxial coupler with a door-knob are shown.

The resonant frequencies and field distribution with the assigned boundary condition including the gun cavity and about a half of the coaxial coupler (without the door-knob) were computed using SUPERFISH in the Standing Wave (SW) mode. Starting from the geometry optimised with SUPERFISH, the door-knob and waveguide part was added and then the field inside the cavity calculated with CST Microwave Studio. It was observed that the axial field flatness between the first (half) and second (full) cells changed by about 30% after adding the door-knob and the waveguide part (Fig. 5). The extra volume added by the door-knob reduced the relative electric field in the second cell and shifted the resonant frequency towards the higher side. Almost the same amount of field balance change was also found for the case with the original DESY coupler design. The field distribution and resonant frequencies would not deviate from that computed by SUPERFISH if the coaxial coupler was weakly coupled to the gun cavity. As we were aiming for critical coupling (β = 1), the presence or absence of the door-knob significantly influences the field distribution. Therefore, to obtain the required field flatness (4% higher at the first cell) and optimal coupling at the design frequency, the computations had to be carried out with the door-knob.

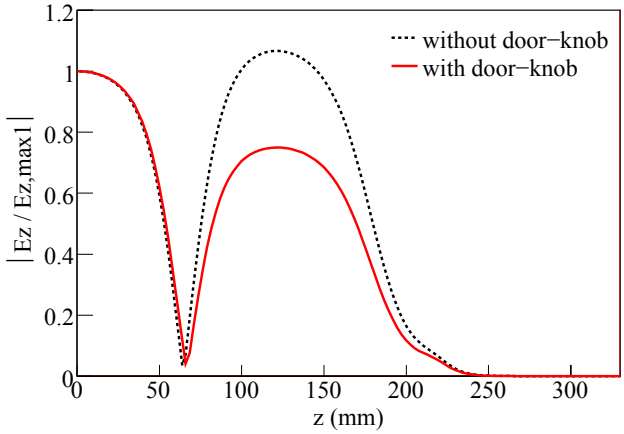

Figure 5: Electric field normalised to the maximum field in first (half) cell along the axis of the gun with coaxial coupler alone (dotted black) and after adding the door-knob (solid red) part to it. The gap between the centre of the cavity exit iris and the nose of the coupler inner antenna was 22 mm.

It took several iterations to optimise the field flatness and the coupling at the same time. To study the coupling between the door-knob and the gun cavity, Time Domain (TD) simulations were performed with the lossy (OFHC copper) metal walls. In order to have better frequency resolution, the simulations were done over a shorter frequency range and a large number of frequency samples. The gap was a very crucial parameter which determined the coupling and the relative field in the second cell for the particular location of the shorting plane in the waveguide. When we started from a balanced field case we found that the doorknob was under coupled and the gap between the centre of the cavity exit iris and the nose of the coupler inner antenna needed to be reduced to increase the coupling. This reduced the electric field in the second cell requiring a change in the cell diameters to increase the field strength. This in turn increased the coupling further and might result in over coupling. The gap was optimised over several such iterations to have the desired field balance in the cells and critical coupling. Figure 6 shows the S11 in the 0- and π-modes for a 31 mm gap. The mode separation between the two modes was 4.5 MHz. The larger the diameter of the iris, the bigger the mode separation. With the cavity with a larger iris diameter, the beam acceleration by the RF field near the beam axis is not as effective as for this case and, as the result, the beam transverse emittance was found to increase according to ASTRA [15] simulation. Figure 7 shows the electric field normalised to maximum

field in the first cell for the π mode along the beam axis for the optimised condition.

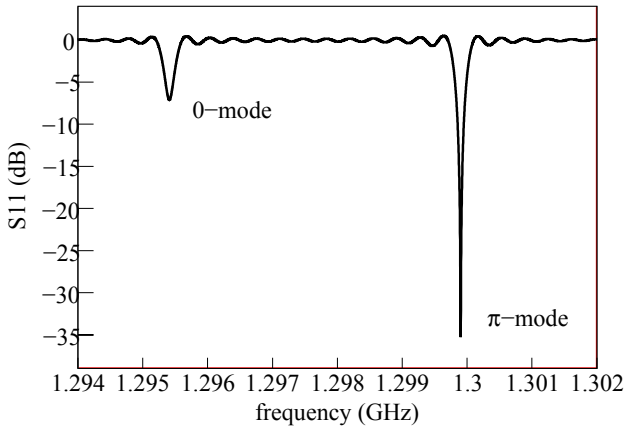

Figure 6: S11 in the frequency range including the 0- and π-modes. The π-mode is critically coupled with a 3.1 mm gap between the centre of the cavity exit iris and the nose of the coupler inner antenna. The mode separation is 4.5 MHz.

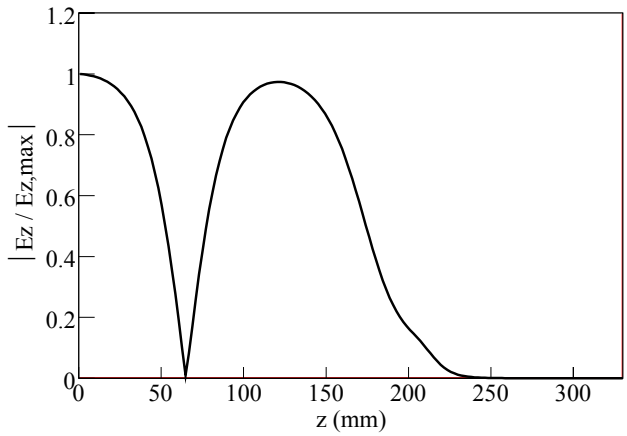

Figure 7: Electric field normalised to the maximum field in the first cell for the π mode in the critically coupled gun cavity with the door-knob.

DISCUSSION

The designed NLS gun will be able to operate with 77 kW RF average power even though the average power is higher than that of the PITZ gun [16] which has been experimentally demonstrated. On the other hand, the NLS gun will have a shorter RF pulse length, 15 μs, and the temperature rise during an RF pulse will only be in the range of a few degrees. Such a temperature rise during the RF pulse should not result in the cavity damage due to fatigue or change the cavity quality factor significantly. The coupling between the RF gun and coupler was investigated numerically. An optimum shape of the door-knob and the gap length between the centre of the cavity exit iris and the nose of the coupler inner antenna were found. This new design will be tested with an aluminium prototype.

ACKNOWLEDGEMENTS

The authors thank K. Floettmann, S. Schreiber (DESY), M. Jensen and R.P. Walker (DLS) for valuable discussions. The mechanical design work by T. Farr, J. Kay, A. Peach and L. Zaja is appreciated.

REFERENCES

[1] R. Walker et al., "A Proposed New Light Source Facility for the UK", PAC'09, TU5RFP022; and more information at http://www.newlightsource.org/.
[2] J.-H. Han, "Design of a Normal Conducting L-band Photoinjector", PAC'09, MO6RFP059.
[3] R. Bartolini et al., "A 1 keV FEL Driven by a Superconducting Linac as a Candidate for the UK New Light Source", PAC'09, TU5RFP062.
[4] http://www.xfel.eu/.
[5] S. Schreiber et al., "Operation of FLASH at 6.5 nm Wavelength", EPAC'08, p. 133 (2008); and more information at http://flash.desy.de/.
[6] K. Floettmann et al., "RF Gun Design for the TESLA VUV Free Electron Laser", Nucl. Instr. and Meth. A393, 93 (1997).
[7] ANSYS v.11, ANSYS, Inc., http://www.ansys.com.
[8] CST Microwave Studio®, http://www.cst.com.
[9] J.-H. Han and H. Huang, "Numerical Study of the RF Heating of an L-Band Gun", PAC'09, MO6RFP060.
[10] J.H. Billen and L.M. Young, "Poisson Superfish", LAUR-96-1834.
[11] D. Pritzkau, "RF Pulsed Heating", Ph.D. Thesis, SLAC-R-577 (2001).
[12] P.B. Wilson, "Scaling Linear Colliders to 5 TeV and Above", SLAC-PUB-7449 (1997).
[13] V. Paramonov et al., "A Pulsed RF Heating Particularities in Normal-Conducting L-Band Cavities", LINAC'06, THP033, p. 646 (2006).
[14] V.V. Paramonov and A.K. Skasyrskaya, "Pulsed RF heating simulations in normal-conducting L-Band Cavities", TESLA-FEL Report 2007-04 (2007).
[15] K. Floettmann, A Space Charge Tracking Algorithm (ASTRA), http://www.desy.de/~mpyflo.
[16] S. Rimjaem et al., "Tuning and Conditioning of a New High Gradient Gun Cavity at PITZ", EPAC'08, p. 244 (2008).